Statistical Pattern Analysis of Partial Discharge Measurements for Quality Assessment of Insulation Systems in High-Voltage Electrical Machinery

Birsen Yazici, *Member, IEEE*

***Abstract*—In this paper, we present a new statistical analysis method of phase-resolved partial discharge (PD) measurements for the quality assessment of electrical insulation in high-voltage machinery. The method is based on a supervised classification approach which utilizes histogram similarity analysis. The motivation for choosing histogram similarity analysis is twofold. First, the phase-resolved PD measurement itself is, in fact, a two-dimensional histogram. Therefore, a histogram-matching-based approach suits the very nature of the data. Second, histogram similarity analysis combines the typical statistical parameters, used in PD analysis, in a statistically powerful and rigorous way. In our study, we utilize various histogram types and similarity analysis, including correlation, chi-square, and Kolmogorov–Smirnov tests. Further, we propose a postprocessing method to quantify the accuracy of classification results which enables the user to make soft decisions. Our experimental study on laboratory samples demonstrates that the method shows strong potential in detection and classification of insulation defects. The results from our study suggest that the proposed method provides a powerful, general, and mathematically simple approach to the analysis of phase-resolved PD measurements.**

***Index Terms*—High voltage, histogram similarity, partial discharge (PD) analysis, quality assessment.**

I. Introduction

PARTIAL discharge (PD) analysis has been established as a reliable diagnostic tool to asses the insulation systems for their integrity and design deficiencies. Interpretation of the PD patterns can reveal the source and the reason for its occurrence and, therefore, has been used as a condition monitoring and quality control tool by the manufacturing industry (se [1], [13], and references therein). For many years, the interpretation was performed by human experts. In recent years, advancement of computer hardware and pattern recognition techniques has provided automation and improvement of the PD interpretation process. As a result of the computer-aided processing, massive amounts of PD measurements can be interpreted efficiently and reliably. Among the well-known pattern recognition methods applied to PD analysis are expert systems, neural networks, fuzzy classifiers, fractal models, and statistical methods, among others [2]–[5]. For more recent publications and review, see [10]–[13].

This paper presents a quality assessment method for insulation systems in high-voltage electrical machinery. The proposed quality assessment method can be utilized to evaluate the integrity and the design deficiencies of insulation systems during the manufacturing process. The preliminary study on the experimental design and comparison with other techniques was reported in [6]. Since then, the method has been commercialized [7].

In phase-resolved PD measurement data, PD pulses are grouped by their phase angle with respect to the 60-Hz sine wave. Consequently, the voltage cycle is divided into phase windows representing the phase angle axis from 0° to 360°. In our measurement setup, the PD observations takes place over several voltage cycles and the number of occurrences of individual PD events is recorded for each phase window. Hence, the way in which the data are acquired motivates a histogram-based statistical analysis of PD patterns. In the proposed analysis method, phase-resolved PD measurement data are viewed either as a two-dimensional (2-D) histogram in which the two axes consist of phase windows and PD magnitude or as a collection of one-dimensional (1-D) histograms in which the axis consists of PD magnitude.

For quality assessment of high-voltage insulation, a set of PD training measurements are acquired from good and defective insulation equipment. A representative PD measurement and a threshold value are determined for each insulation quality class by using histogram similarity analysis. The quality class representatives and thresholds are then stored in a data base to be used as baselines for normal and defective insulation during the testing stage. In the testing stage, PD measurement is acquired from unknown quality insulation equipment and the distance between the class representatives and the data is measured using histogram similarity measures. If the distance is within the limits of the normal insulation threshold, it is tagged as "good," otherwise, it is tagged as "defective."

The remainder of this paper is organized as follows. In Section II, we introduce the histogram similarity measures. In Section III, we discuss how histogram similarity measures can be utilized as an insulation quality assessment tool. In Sections IV–VII, we discuss preprocessing, training, testing, and postprocessing stages of the method. In Section VIII, we present testing setup and experimental design. In Section IX,

Paper IPCSD-04-043, presented at the 2003 IEEE International Symposium on Diagnostics for Electrical Machines, Power Electronics and Drives, Stone Mountain, GA, August 24–26, and approved for publication in the IEEE TRANSACTIONS ON INDUSTRY APPLICATIONS by the Electric Machines Committee of the IEEE Industry Applications Society. Manuscript submitted for review February 26, 2003 and released for publication July 1, 2004.

The author is with the Department of Electrical, Computer, and Systems Engineering, Rensselaer Polytechnic Institute, Troy, NY 12180 USA (e-mail: yazici@ecse.rpi.edu).

Digital Object Identifier 10.1109/TIA.2004.836174

0093-9994/04$20.00 © 2004 IEEE

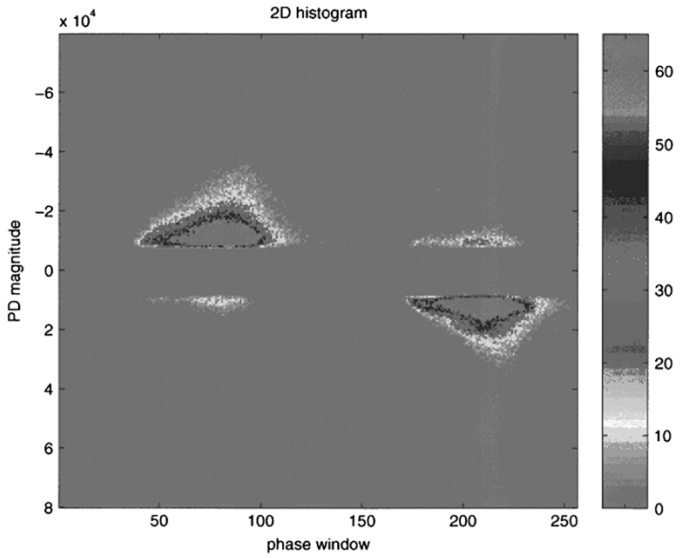

Fig. 1. 2-D histogram for a phase-resolved PD measurement.

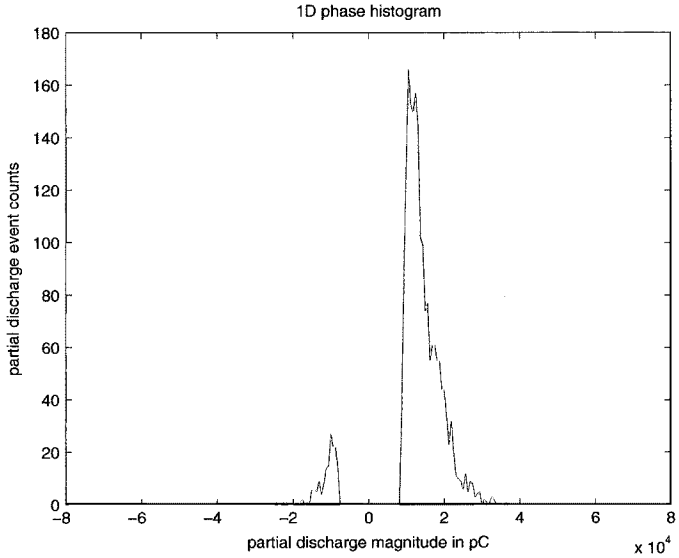

Fig. 2. 1-D phase histogram of PD measurements for a given phase window.

we present numerical results demonstrating the performance of the proposed analysis methods. Finally, in Section X, we briefly discuss further items of interest in the context of insulation quality assessment and conclude the paper.

II. PD Data as a Histogram and Histogram Similarity Measures

A. Histogram Types

In a phase-resolved PD measurement, PD observation takes place over several voltage cycles and the PD pulses are digitally recorded by their phase angle with respect to a single voltage cycle. Therefore, a phase-resolved PD measurement is a 2-D histogram of PD events with respect to discharge magnitude and phase angle. Hence the very nature of the data motivates a histogram based statistical analysis. In this study, phase-resolved PD data are treated as four different kinds of histograms.

- The PD measurement itself is a 2-D histogram. The phase window and the PD magnitude form the two dimensions of the histogram. The joint probability mass function of phase windows and PD magnitudes can be computed by normalizing the histogram to unit area. In our discussion, we shall refer to this histogram as the "2-D histogram." Fig. 1 shows a typical 2-D histogram obtained from our data acquisition system. Note that the voltage cycle is divided into 256 phase windows, each window corresponding to 1.4°.
- For a given phase window, the number of occurrences of individual PD pulses provides a histogram of PD magnitudes. Hence, phase-resolved PD measurements can be viewed as a collection of 1-D histograms in which the dimension is the PD magnitude. The minimum width for the phase window is chosen 1.4 degrees. In our discussion, we shall refer to this collection of histograms as the "1-D phase histograms." Fig. 2 shows a 1-D phase histogram for the phase angle 138.6°–140°.
- To simplify the analysis, one can consider only the total number of occurrences for each phase window or PD magnitude, i.e., the sum of the individual PD events for each phase window or for each PD magnitude. We shall refer to the histogram obtained by the sum of the individual PD events for each phase window as the "X-marginal histogram," and the histogram obtained by the sum of the individual PD events for each PD magnitude as the "Y-marginal histogram." Figs. 3 and 4 show X- and Y-marginal histograms of a phase-resolved PD measurement.

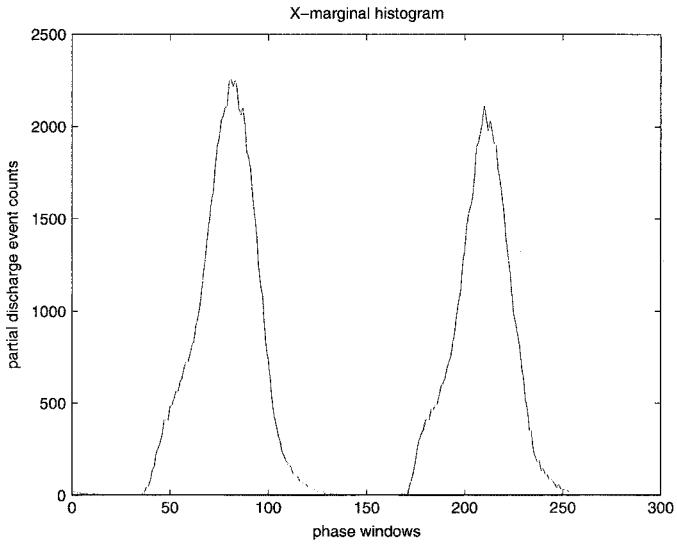

Fig. 3. X-marginal histogram of a phase-resolved PD measurement.

B. Histogram Similarity Measures

In this study, we used four histogram similarity measures to asses the discrimination value of each one under different circumstances. These measures are as follows:

- sample correlation;
- Kolmogorov–Smirnov distance 1 and 2;
- chi-square test.

Sample correlation regards two histograms as vectors and checks if the two histograms are parallel geometrically. Kolmogorov–Smirnov distances compares two histograms with

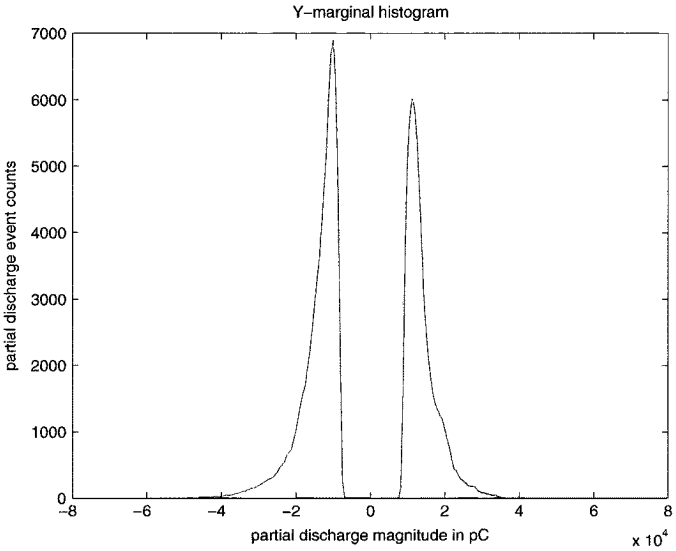

Fig. 4. Y-marginal histogram of a phase-resolved PD measurement.

respect to point shifts and chi-squares test compares two histograms with respect to the number of observations.

To keep the notation simple, we shall describe these measures for a 1-D histogram. The 2-D description is a straightforward extension. To facilitate our discussion, let us introduce some notations.

Probability mass function or normalized histogram

$$P(i) = \frac{h(i)}{A}, \qquad i = 1, \ldots, N \tag{2.1}$$

where

$h(i)$ number of events whose intensity is i;
A total number of events in the measurement set;
N number of bins in the histogram.

1) Cross-correlation value

$$Cr = \frac{\sum_{i=1}^{N} (P_1(i) - \mu_1)(P_2(i) - \mu_2)}{\sqrt{\sum_{i=1}^{N} (P_1(i) - \mu_1)^2 \sum_{i=1}^{N} (P_2(i) - \mu_2)^2}} \tag{2.2}$$

where μ_i is the mean value of the probability density function $P_i,\ i = 1, 2 \ldots$

2) Kolmogorov–Smirnov distance [8]—cumulative distribution function

$$H(k) = \sum_{i=1}^{k} P(i), \qquad k = 1, \ldots, N. \tag{2.3}$$

a) Kolmogorov–Smirnov distance 1

$$\mathrm{KS1} = \max_k |H_1(k) - H_2(k)|. \tag{2.4}$$

The distribution of the Kolmogorov–Smirnov statistics in the case of null hypothesis (data sets drawn from the same distribution) can be calculated, thus giving the significance of any observed nonzero value of KS1. The function that enters the calculation of the significance can be written as the following sum:

$$Q_{\mathrm{KS1}}(\lambda) = 2 \sum_{j=1}^{\infty} (-1)^{j-1} e^{-2j^2\lambda^2}. \tag{2.5a}$$

In terms of this function, the significance level of an observed value of KS1 (as a disprove of the null hypothesis that the distributions are the same) is given approximately by the formula [14]

$$\text{Probability (observed} < \mathrm{KS1}) = Q_{\mathrm{KS1}}([\sqrt{A_e} + 0.12 + 0.11/\sqrt{A_e}]\mathrm{KS1}) \tag{2.5b}$$

where A_e is the effective number of data points given by

$$A_e = \frac{A_1 A_2}{A_1 + A_2}. \tag{2.5c}$$

A_1 and A_2 are the number of data points in the first and second distributions, respectively. For the 2-D Kolmogorov–Smirnov test the probability that the observed test statistics exceeds KS1 is given by [15]

$$\text{Probability (observed} < \mathrm{KS1}) = Q_{\mathrm{KS1}}\left(\frac{\mathrm{KS1}\sqrt{A_e}}{[1 + \sqrt{1 - r^2}(0.25 - 0.75/\sqrt{A_e})]}\right) \tag{2.5d}$$

where r is the correlation coefficient defined in (2.2).

b) Kolmogorov–Smirnov distance 2

$$\mathrm{KS2} = \sum_{k=1}^{N} |H_1(k) - H_2(k)|. \tag{2.6}$$

3) Chi-square test

Let $h(i) i = 1, \ldots, N$ be a histogram observed in an experiment and $P(i), i = 1, \ldots, N$ be a known probability mass function. We want to know whether $h(i)$'s are drawn from the population represented by the $P(i)$'s. We measure the distance between the two distributions via the chi-square statistics [8]

$$\chi^2 = \sum_{i=1}^{N} \frac{(h(i) - AP(i))}{AP(i)} \tag{2.7}$$

where A is the total number of observations in the experiment. If $h(i)$'s are indeed drawn from the population represented by $P(i)$'s, then it can be shown by the central limit theorem that as $A \to \infty$, each term in the summation of (2.6), is the square of a Gaussian random variable with zero mean and unit variance. Therefore, χ^2 is a random variable with chi-square distribution. A large value of χ^2, e.g., $\chi^2 \gg N$, indicates that it is rather unlikely that the two distributions represented by $h(i)$'s and $P(i)$'s are the same.

Let $\Pr(\chi^2 > C \,|\, N)$ be the probability that the chi-square statistic is at least C, given that there are N bins in the histogram and that $h(i)$'s are drawn from the population represented by $P(i)$'s. The value of $\Pr(\chi^2 > C \,|\, N)$ can be computed by the incomplete gamma function

$$\text{Probability}\,(\chi^2 > C \,|\, N) = \frac{\int_{C/2}^{\infty} e^{-x} x^{N/2-1} dx}{\int_{0}^{\infty} e^{-x} x^{N/2-1} dx}. \tag{2.8}$$

Chi-square test for two histograms

Since we really do not know the "true" probability mass functions of the PD events, what we implement is a modified chi-square test which checks whether the two measurements $h_1(i), i = 1, \ldots, N$, and $h_2(i), i = 1, \ldots, N$ are drawn from the same population by some unknown probability distribution function. It can be shown in this case that the chi-square statistics is given by

$$\chi^2 = \sum_{i=1}^{N} \frac{(\sqrt{A_2/A_1}h_1(i) - \sqrt{A_1/A_2}h_2(i))}{h_1(i) + h_2(i)} \qquad (2.9)$$

where $\sum_{i=1}^{N} h_1(i) = A_1$ and $\sum_{i=1}^{N} h_2(i) = A_2$.

In our implementation, $h_1(i)$ is the first histogram, and $h_2(i)$ is the second histogram of PD events. Note that if $h_1(i) = h_2(i) = 0$ for some bin i, then the corresponding term is dropped in the summation in (2.9).

III. Quality Assessment of the Insulation System

The proposed quality assessment method is a "supervised" approach, that is, the type and the number of insulation defects is predetermined. The method can be utilized for *detection*, as well as *identification* of insulation defects. The "detection" involves an automatic decision making to determine whether a given test insulation is good or not. The "identification," on the other hand, involves detection, as well as classification, of the insulation defect to one of the known defect classes.

As more information is provided to the system, improved defect detection and identification can be achieved. For defect detection, only a set of PD measurements representing a good insulation system is needed. For identification, however, PD measurements from the defect classes are needed. These defect classes may be: 1) suspended metal particulate in insulation; 2) armor degradation; 3) conductor/insulator delamination; 4) insulator/insulator delamination; or 5) insulator/armor delamination, among others. The outcome of such a quality assessment system is one of the following: 1) good insulation; 2) defective insulation with known defect type; and 3) defective insulation with unknown defect type.

The method consists of four stages: preprocessing, training, testing, and postprocessing. In the preprocessing stage, the PD data are subjected to signal conditioning methods, such as gain normalization, phase shifting, and noise suppression. In the training stage, the features of defective and good insulation are learned from a set of so-called training data. The learning process involves feature extraction from raw data and statistical analysis. The statistical analysis of the features leads to a set of representatives and thresholds for each class. The representatives of each class along with the thresholds are stored in a data base to be used as baselines during the testing stage. In the testing stage, features are extracted from a test PD data coming from an unknown insulation quality and a statistical distance between the representatives of each class and the features is computed. The resulting distances are compared with the thresholds in the data base to check whether the test measurement belongs to one of the known classes. In the post processing stage, the decisions from multiple PD measurements are combined to increase the confidence level and a probability is associated with each decision to quantify the accuracy of the process. Fig. 5 illustrates the major stages of the proposed quality assessment process. Each stage is discussed in more detail in the following sections.

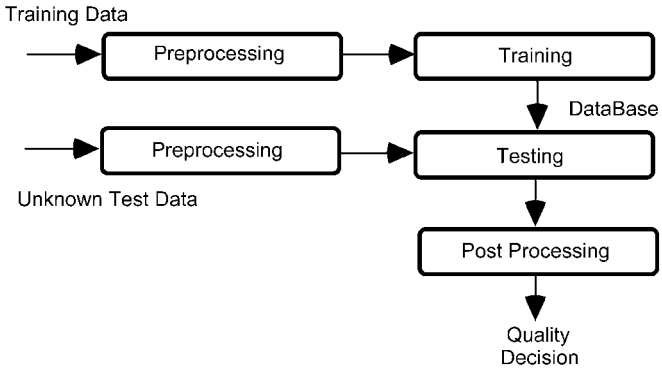

Fig. 5. Block diagram of the quality assessment method.

A. Preprocessing

In this stage, the raw PD data are processed: 1) to convert from bipolar mode to a unipolar mode; 2) to adjust the phase with respect to supply voltage; and 3) to normalize with respect to gain factor. Also, as a part of the PD computer aided diagnosis system, digital filtering can be applied to suppress periodic noise in the measurements, if needed. For example, excitation noise often results in spikes superimposed on the PD data [9]. In our study, such a noise was removed by standard digital notch filtering in the frequency domain.

B. Training

The block diagram of the training process is illustrated in Fig. 6. In this section, we shall explain each step in more detail.

It is well-known empirically that the low-count high-magnitude PD events contain more discrimination information than the low-magnitude high-count PD events [6]. During the feature extraction process, in order to highlight the relative importance of the low PD counts, we take the logarithm of the PD event counts and thereby suppress the effect of the high-count low-magnitude events. Additionally, the resulting data can be thresholded to eliminate low-magnitude events.

After feature extraction, a representative is determined for each class by averaging the PD data. Let R_i denote the representative of the class i, $i = 1, \ldots, L$ and $P_i^j, j = 1, \ldots, N_i$ be the jth member of the class i where L is the total number of classes and N_i is the number of samples available for class i. Next, an intra-class distance between the class representative R_i and each of its members P_i^j is calculated by using the histogram similarity measures introduced in Section II

$$D_i^j = d\left(P_i^j, R_i\right), \qquad j = 1, \ldots, N_i; \quad i = 1, \ldots, L \qquad (5.1a)$$

where d stands for one of the histogram similarity measures. Note that in the case of 1-D phase histograms, the distance function is a vector in which each entry is the distance between the member and the reference 1-D phase-resolved histograms

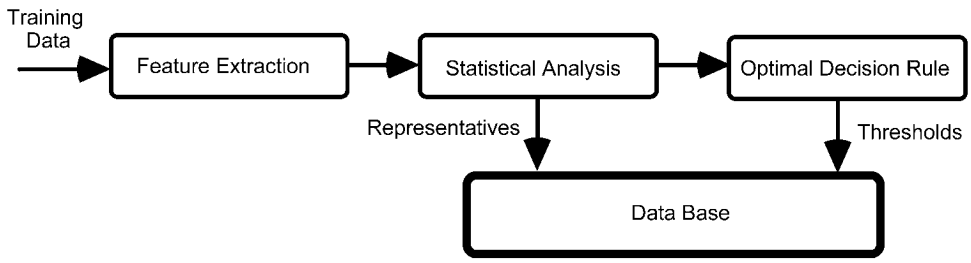

Fig. 6. Block Diagram of the Training Stage.

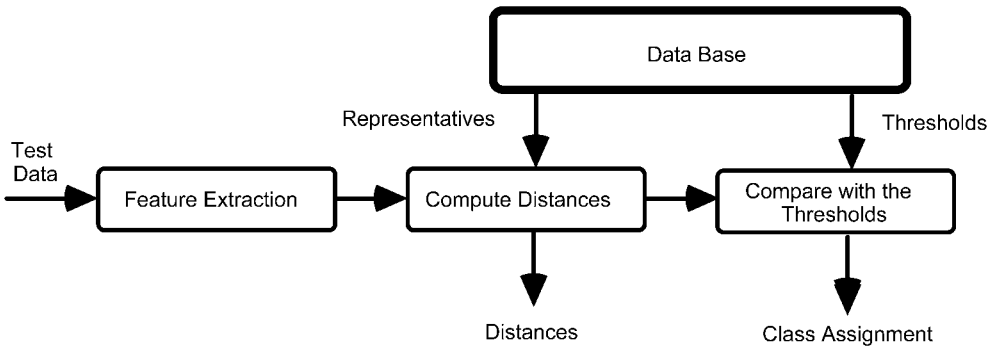

Fig. 7. Block diagram of the testing stage.

for each phase window. To clarify the difference, we introduce vector notation for the 1-D phase histograms

$$D_i^j(\omega) = d\left(P_i^j(\omega), R_i(\omega)\right), \qquad \omega = 1, \ldots, 256 \quad (5.1b)$$

where ω corresponds to the phase window.

In order to obtain the optimal radius for each class, the sample mean and standard deviation of the distances within each class are calculated. For the 2-D histograms, the intra-class mean radius and standard deviation are given as follows:

$$\bar{D}_i = \frac{1}{N_i}\sum_{j=1}^{N_i} D_i^j \quad (5.2a)$$

$$\sigma_i = \sqrt{\frac{1}{N_i}\sum_{j=1}^{N_i}\left(D_i^j - \bar{D}_i\right)^2}. \quad (5.2b)$$

For the 1-D phase histograms the intra-class mean radius and standard deviation are given by

$$\bar{D}_i(\omega) = \frac{1}{N_i}\sum_{j=1}^{N_i} D_i^j(\omega) \quad (5.3a)$$

$$\sigma_i(\omega) = \sqrt{\frac{1}{N_i}\sum_{j=1}^{N_i}\left(D_i^j(\omega) - \bar{D}_i(\omega)\right)^2}, \qquad \omega = 1, \ldots, 256. \quad (5.3b)$$

Next, an α unit standard deviation tolerance is allowed for each class radius. Note that in case of Gaussian distribution of intra-class distances, α is typically chosen to be 2 to provide a 99% confidence interval. However, in our scheme, it is kept as an input parameter to allow the user to utilize one's engineering judgment in setting the tolerance. The class radii $\tau_i, i = 1, \ldots, L$, for the 2-D and 1-D histograms are given as follows:

$$\tau_i = \bar{D}_i + \alpha\sigma_i \quad (5.4a)$$

$$\tau_i = \sum_{\omega=1}^{256} \bar{D}_i(\omega) + \alpha\sigma_i(\omega), \qquad \omega = 1, \ldots, 256. \quad (5.4b)$$

Note that in both 2-D and 1-D histograms, the class radius is given by a scalar value. Finally, the representative and the threshold of each class $\{R_i, \tau_i\}$ are stored in the data base.

IV. Testing

The major steps of the testing process are illustrated in Fig. 7. Similar to the training process, the test data are first subjected to the operations discussed in the preprocessing stage and feature extraction process described in the training stage. Next, using one of the histogram similarity measures, the distance between the test feature T and the reference of each class R_i is computed. For the 2-D histogram, the distance is given by a scalar quantity while for the 1-D phase histograms, it is given by a vector quantity

$$\Delta_i = d(T, R_i), \qquad i = 1, \ldots, L \quad (6.1a)$$

$$\Omega_i(\omega) = d(T(\omega), R_i(\omega)), \qquad \omega = 1, \ldots, 256; \quad i = 1, \ldots, L. \quad (6.1b)$$

where L is the total number of classes. In order to compare the vector quantity, (6.1b), with a scalar threshold, we compute a cumulative distance by summing the quantity in (6.1b) over all the phase windows

$$\Delta_i = \sum_{\omega=1}^{256} \Omega_i(\omega). \quad (6.2)$$

Next, we check if the distance between test feature and the references of each class Δ_i is less than the class threshold τ_i. If the distance Δ_i is greater than all the thresholds, $\tau_i, i = 1, \ldots, L$, the test measurement is tagged as defective, but of unknown defect type. If the distance Δ_i is less than one or more thresholds, the test measurement is assigned to the class for which the distance between the reference and test feature is minimum. If the assignment is the class of good insulation, the measurement is tagged as nondefective.

To improve the accuracy of our decision making, we repeat this testing scheme for multiple PD measurements for each insulation equipment. Decisions obtained from each measurement and the distances of the test features to the class representatives are fed to the postprocessor to finalize the decision on the insulation equipment.

V. Postprocessing

In the postprocessing stage, there are two major tasks: 1) classify the insulation equipment by combining the decisions from each test PD measurement and 2) associate a probability to each decision reflecting the accuracy of the classification process. We shall start with the second task since making a final decision on the insulation equipment depends on the accuracy of each decision made on individual PD measurements. Recall that during the testing stage, a distance between the test feature and the representative of each class is computed

$$\Delta_i = d(T, R_i), \qquad i = 1, \ldots, L. \tag{7.1}$$

The distance of the test feature to a class representative is quantified in terms of unit standard deviation of the class. Relative comparison of these distances determines the accuracy of the final decision. To compare these decisions, we compute the probability distribution of the test statistics, namely, the test statistics of the chi-square, Kolmogorov–Smirnov 1 and 2 tests, and correlation test. The test statistics of the chi-square and Kolmogorov–Smirnov 1 tests are provided in (2.5b), (2.5d) and (2.8), respectively. For the test statistics of the correlation and Kolmogorov–Smirnov 2 tests, we assume Beta distribution with parameter β. In particular, we employed the following version of the Beta distribution:

$$f(\Delta) = \begin{cases} (1-\beta)\left(1 - \frac{\Delta}{\gamma}\right)^{-\beta}, & 0 \le \Delta < \gamma \\ 0, & \Delta \ge \gamma. \end{cases} \tag{7.2}$$

Note that

$$\text{Probability}\ (\Delta > C) = \left(1 - \frac{C}{\gamma}\right)^{-\beta}. \tag{7.3}$$

Therefore, when the distance is 0, i.e., $\Delta = 0$, the probability is 1, and when the distance is greater or equal to γ, the probability is 0. Beta distribution on the correlation and Kolmogorov–Smirnov test are reasonable assumptions. Because, if the distance between the test feature and a class representative is either 0, or an order of a magnitude larger, such as α^2, it is reasonable to assume that the conditional probability of that particular class given the measurements is either very high or very low. In the case of 0 distance, Beta distribution suggests that the test measurement belongs to the class with probability 1, and in the case of α^2 or larger distance, the probability that the test measurement belongs to that class is 0.

There are two user-controlled parameters in the Beta distribution (7.2), namely, γ and β. The parameter γ controls the threshold beyond which the probability that a measurement coming from a particular class of distance γ or larger is 0. This distance can be set to an order magnitude larger than the threshold α, such as α^2 unit standard deviation or can be determined experimentally during the training stage. The parameter β controls the confidence in the class identification power of the testing scheme. This parameter should be set to a value so that 80% or more values should be correctly classified. This value can be determined empirically during the training stage. If an 80% class identification level is assumed, β is given by

$$\beta = -\ln 0.8 / \ln(1 - \alpha/\gamma) \tag{7.4}$$

or, more generally, β can be chosen so that Probability $(\mathrm{D} > \alpha)$ is equal to the confidence level in percentage. Fig. 8 shows how the proposed probability mapping function behaves for typical values of $\gamma = \alpha^2$ and β given in (7.4).

Next, we combine the class assignments and the associated probability values obtained from multiple PD measurements to get a final class assignment and a probability value for a given insulation equipment. The steps of this process can be summarized as follows.

- Assign a probability value to each PD measurement describing the likelihood of the measurement belonging to each class in the database. Let $p_i^j, j = 1, \ldots, M_i$ and $i = 1, \ldots, L$ be the probability that the measurement j belongs to class i where M_i is the number of measurements collected from the insulation equipment and L is the number of classes.
- Define

$$\bar{p}_i = \frac{1}{M} \sum_{j=1}^{M} p_i^j, \qquad i = 1, \ldots, L \tag{7.5}$$

as the probability that the insulation equipment belongs to class i with probability $\bar{p}_i$. Finally, the insulation equipment is assigned to the class with the highest overall probability, i.e.,

$$\hat{i} = \mathrm{Argmax}_i \bar{p}_i \tag{7.6}$$

where $\hat{i}$ is the class label at which $\bar{p}_i,\ i = 1, \ldots, L$ is maximum.

VI. Design of Experiments

This paper covers several types of defects on stator bars:

1) suspended metallic particles in the groundwall insulation;
2) slot armor degradation;
3) corona suppressor degradation;
4) insulation–conductor delaminations;
5) insulator–insulator (bound) delaminations;
6) "white" bars (puffed insulation).

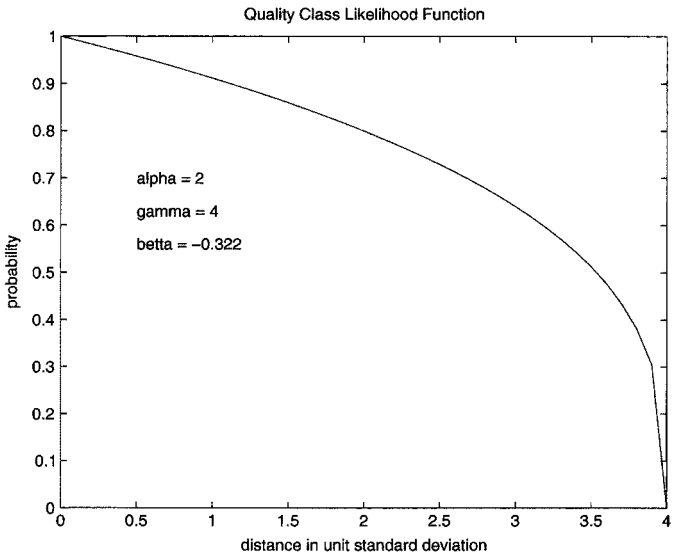

Fig. 8. Quality class likelihood function.

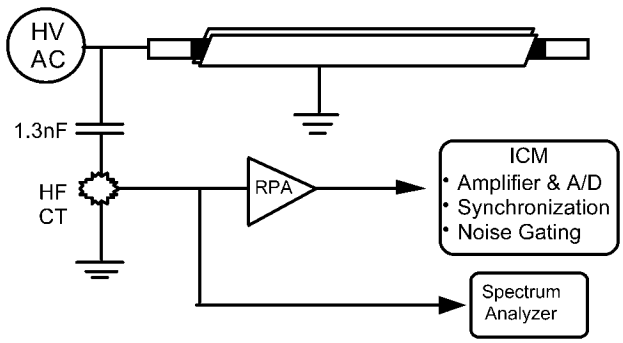

Fig. 9. PD testing configuration.

Each of these defect types has implications for either the manufacture of individual bars or machines, as well as actual field degradation phenomena. Each bar was subjected to a specific, sequential protocol to investigate the effects of voltage application on new bars, the effects of hipot, and the effect of a single thermal cycle on the PD patterns.

The test configuration is shown in Fig. 9. A 60-Hz corona-free high-voltage supply energized model generator stator bars. The bars were placed in a simulated stator slot and held firmly with C-clamps. The slot was made of either aluminum or steel plates cut to fit the slot section of the bars. A 1.3-nF ceramic coupling capacitor was used as a coupling impedance. Placed on the ground strap to the coupling capacitor, a high frequency current transformer collected the PD signals. The signals were monitored by a phase-resolved PD acquisition system. The bandwidth of data collection was 100 k to 800 kHz. Data was collected for 30 s for each pattern.

The bars were a collection of both genuine stator bars (with end-arms) and straight quality control (QC) bars. Construction of the QC bars is as follows: to bare copper bars, an internal grading of conductive tape was laid; 10 layers of mica tape were laid next; to this was laid the external armor; on the ends, one layer of corona suppressor tape was used; the bars were compounded according to normal factory conditions. The bars were designed for a 13.8-kV machine application (8 kV line-to-ground). Corona suppressors were more than 7 in long, making the bars suitable for PD testing up to 35 kV. The bars were generally tested at line-to-ground voltages. Table I shows a collection of the bars and the defects. Additional stator bars were of similar construction.

TABLE I
MODEL DEFECT BARS

Bar Name	*Defect Type*
TT539B	None
Grade	TT539 Later: disconnected corona suppressor
TT540B	None
TT542B	Metal pieces
TT547B	No internal grading
TT548B	No internal grading
TT555B	Bared copper/insulation delamination
TT595B	White bar (puffed) insulation
2E18	750 thermal cycles 14,000 Hr VE
2G18	Painted slot armor w/end-arm (control)
2G17	Painted slot armor w/end-arm (degraded)

A. Good Bars

In order to establish a baseline, three "good" bars were produced. Typical phase-resolved PD patterns are shown in Fig. 10(a) and (b). The activity pattern is a characteristic "hump" centered in the first and third quadrants. The activity levels are low, with maximum discharges (at 1 pulse/s discharge rates, minimum) of only 91 pC.

There can be noticeable conditioning with voltage application and/or voltage/thermal history. Both the maximum magnitude discharge with at least 1 pulse/s discharge rate $(Q1_{\max})$ and the activity level (count rate at fixed gain) are plotted in Fig. 11 for a representative "good" bar. The activity is initially high (Point A) and conditions over the first 20–40 min. This is believed to be caused by conditioning of various, ubiquitous voids in the insulation. The activity then increases over the next several hours (Point B). This is postulated to be due to activation of the internal grading: it is believed that the internal grading may not be fully activated until subjected to sufficient voltage. This activation is accompanied by electrical activity, detected as internal PD. Finally, the bar conditions to a baseline level (Point C) that the bar will maintain until significant insulation degradation initiates.

If the voltage is removed after several days of electrical conditioning, and subsequently reapplied after a cooldown time, the PD activity will again be high (Point D) and then decay, but the bump phenomenon (Point B) is not observed again. This time, however, conditioning takes about 2 h before a plateau is reached.

If the bar is then subjected to a 1-min hipot at three times rated voltage (the factory specification), the subsequent PD is even lower (Point E). This shows the conditioning effect that hipot testing can have on good bars. In contrast, hipot testing can aggravate some defects in bad bars. This shows the symbiotic relationship that exists between PD and other electrical tests.

If the bar is then subjected to a single thermal cycle (3 h at 155 ∞C), the PD activity is enormous (Point F). This is caused by insulation delamination from the copper due to differences

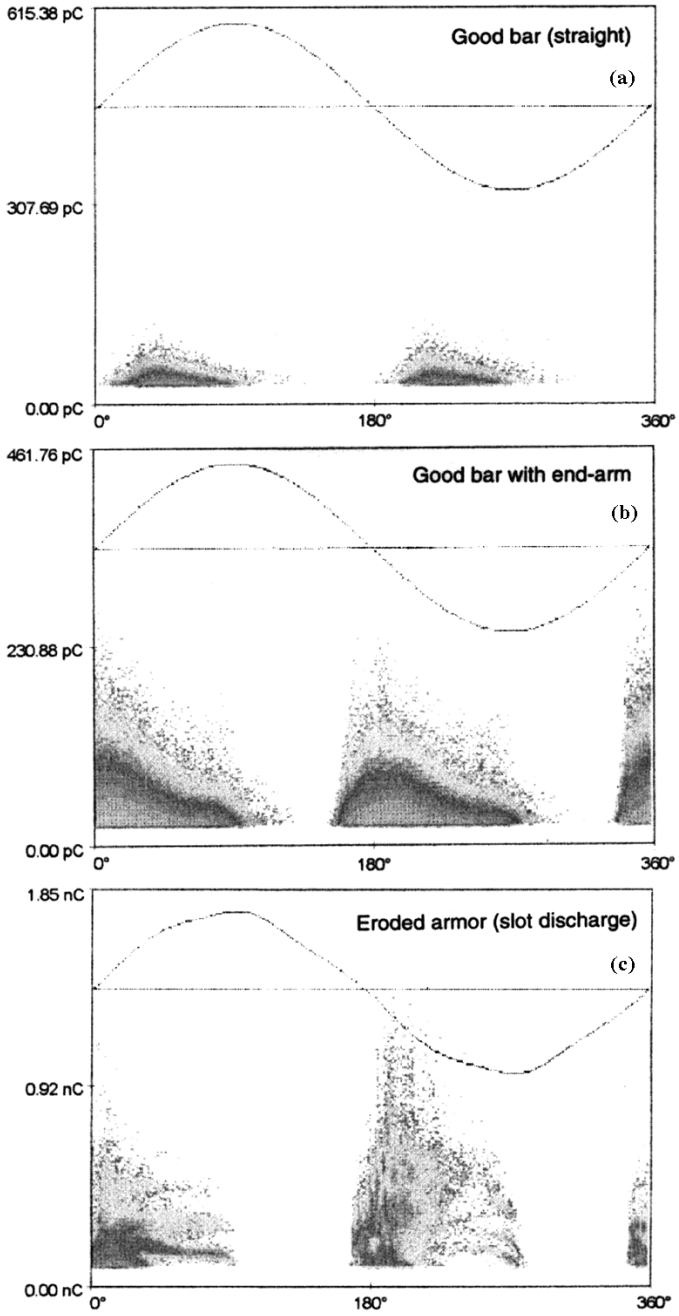

Fig. 10. Representative phase-resolved PD measurements for (a) good bars, (b) good bars with end-arm, and (c) bars with slot discharge.

in the coefficient of thermal expansion. This happens after a new winding or machine is turned on for the first time and then allowed to cool. The activity will condition, but it takes about 10 h. Accordingly, it is important to have machines running at stable load and temperature conditions as long as possible prior to measuring PD activity in order to ensure reliable data. Bars in a machine need significantly more settling-in time due to the compounded effects of thermal cycling and vibration.

B. Slot Armor Degradation

Slot armor degradation is a phenomenon that happens as a result of bars vibrating in the slot. The stator core lamination edges, and sometimes the wedge systems as well, provide an unfriendly, coarse surface. The forces on a bar in a slot are radial and are caused by the currents flowing in the bar. The forces are proportional to the square of the current and cause the bar to oscillate at the second harmonic. As a result, PD activity from this type of defect is often (but not always) load sensitive.

Fig. 10(c) shows a representative phase-resolved PD pattern taken from bar 2G17 that demonstrates the effect of slot armor degradation on PD activity. This bar is a solventless end-section with end-arm. The bar had painted (rather than taped) armor. This is often done when bars are slightly oversized after compounding; the armor tape is removed to fit the bar, and a semiconductive paint is applied instead. This paint does not survive under voltage stress as well as does tape. As a result, the paint eventually erodes, leaving bare insulation exposed to the stator armor. Consequently, electrical discharges occur in the air gap, producing large PD signals and are often accompanied by ozone formation. These discharges are large and are therefore more detrimental to insulation than are other defects. Allowed to progress, the discharges will disintegrate the epoxy from within the wrapped tape, leaving a white, powdery residue (often called "corona dusting").

The differences in PD patterns are striking. The magnitude of PD activity from slot discharge is often very large. In this instance, the activity is five times larger than normal. More characteristic, however, is the shape of the PD pattern. In contrast to the typical "hump" of PD activity seen from the control, slot discharge results in "shelves of activity" or often "squared-off" patterns. In addition, this type of event often results in high frequency signals.

Data taken from hydro generator bars with taped armor showed similar behavior. Hence, in terms of slot discharge PD patterns, there is nothing unique about painted versus taped armor.

It has been suggested that this pattern should shift in phase-space with varying load and/or power factor. An extensive investigation, using currents up to 2500 A, and power factors from leading to lagging by as much as 35° in each direction, showed this not always to be the case. The patterns follow the voltage and did not seem to vary significantly with load. A small change in amplitude was noted, but on a complete stator, this would be insignificant. This load independence is believed to be due to surface roughness of the typical stator bar: a perfectly smooth stator bar might behave differently.

Related to the phase shift of this pattern is the phase shift that occurs due to test voltage. In this test, the position in phase space of the onset of PD activity was monitored as a function of applied voltage. Going from the corona inception voltage (CIV) to 14 kV (rated phase-to-phase voltage), one sees a shift in the position of PD onset from 26° to −35°. This is a shift of over 60°.

C. Corona Suppressor Degradation

Corona suppressor degradation is a phenomenon that often occurs during voltage-endurance (VE) testing but can also occur in service. Phase-to-phase discharges can also cause this degradation. On isolated bars, however, it is sometimes manifested in burnout of the corona suppressor immediately adjacent to

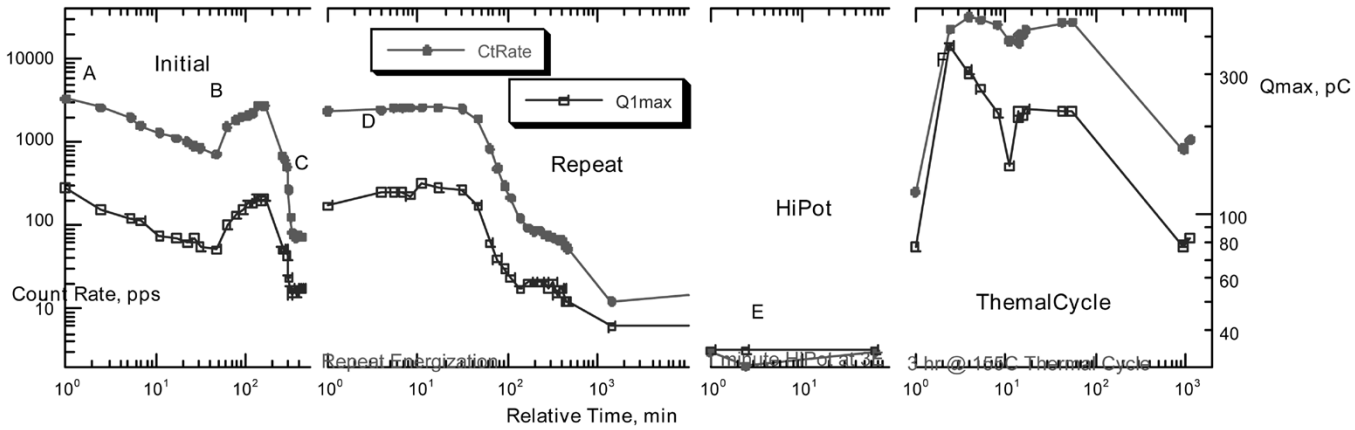

Fig. 11. Bar TT539B (Good Bar) typical aging and conditioning patterns.

the slot armor. This is due to the heat that is generated during voltage application, particularly during VE testing. This results in a disconnected corona suppressor which is accompanied by surface discharges. The results of excessive discharges will produce white powder (corona dusting). Often, this type of damage is only cosmetic and can be repaired.

To expedite this, the corona suppressor on a good bar was disconnected adjacent to the slot section by filing it away. The bar was then put on test and the patterns analyzed. A typical phase-resolved PD pattern is shown in Fig. 12(a). The pattern is readily distinguished from that of normal, internal PD [Fig. 10(a)].

D. Insulation–Conductor Delaminations

Delaminations at the conductor-insulator interface commonly occur in machines that experience many thermal cycles. This defect is particularly prevalent in machines that are used for load peaking. Also, many cogeneration facilities will cycle on a weekly basis and often suffer conductor–insulator delaminations as a result.

To simulate this defect, release agent was used on the bare bar prior to application of the groundwall insulation. The strand insulation is not corona resistant and will degrade in the presence of PD. However, to expedite this process, the strand insulation was removed in several areas by light sanding prior to applying the groundwall insulation. Representative phase-resolved PD plots are shown in Fig. 12(b).

After application of a single hipot, the count rate for this bar more than doubled. Interestingly, however, Q_{max} only increased by about 25%. Neither, however, conditioned significantly afterward. This shows the aggravating effect that hipot tests can have on this defect. The hipot test acted to initiate many new sites of activity (as manifested in the count rate).

E. Insulator–Insulator (Bound) Delaminations

Voids are ubiquitous in high-voltage insulation. Usually, however, these voids are relatively small. Most of these small voids will undergo electrical conditioning whereby the inner surfaces of the voids are covered with semiconductive degradation products. Consequently, the electrically active voids may eventually "turn off." This is part of the conditioning process of normal high-voltage insulation for rotating machinery.

Void "packets" were prepared in freestanding pre-cured insulation. These packets were then incorporated into the insulation during the winding process and located at know positions along the bar. The packets were not located at the edges of the bar as this is difficult to do and often not the location for large voids to occur.

Phase-resolved PD patterns were collected and a representative plot is shown in Fig. 12(c). Not surprisingly, the pattern is strikingly similar to those from a normal (i.e., good) insulation, making discrimination difficult without the aid of sophisticated analysis procedures.

F. "White" Bars (Puffed Insulation)

White bars occur when a stator bar is not completely covered by resin during the VPI process. This results in a bar that is "puffy." This scenario is particularly useful for bar quality control and/or bar quality analysis.

Phase-resolved PD patterns were collected and a representative plot is shown in Fig. 13(a). Not surprisingly, the pattern is strikingly similar to those from a normal (i.e., good) insulation.

G. Suspended Metallic Particles in the Groundwall Insulation

To simulate this effect, three defects were introduced into the same bar, located at three sites: the first defect is a 0.75-in-long 7-mil-diameter magnetic wire buried within the third mica tape layer along a corner, with the wire oriented axially; the second defect is identical to the first except it is located in the fifth mica tape layer; the third defect is a 5-mg piece of steel wool in the seventh mica tape layer along a corner. Infrared and dissipation factor tests were unable to detect the particles. These tests, in addition to a hipot test, indicated that the bar exhibited normal test results.

Phase-resolved PD patterns were collected and a representative plot is shown in Fig. 13(b). Surprisingly, the pattern is very similar to those from a normal (i.e., good) insulation. A single hipot did not noticeably aggravate any discharge quantities or symmetries for this defect.

H. No Internal Grading

Internal grading was introduced in 1992 for generator stator bars by some manufacturer. Consequently, a large fleet of generators in operation does not contain internal grading. While internal grading has been shown to improve voltage endurance

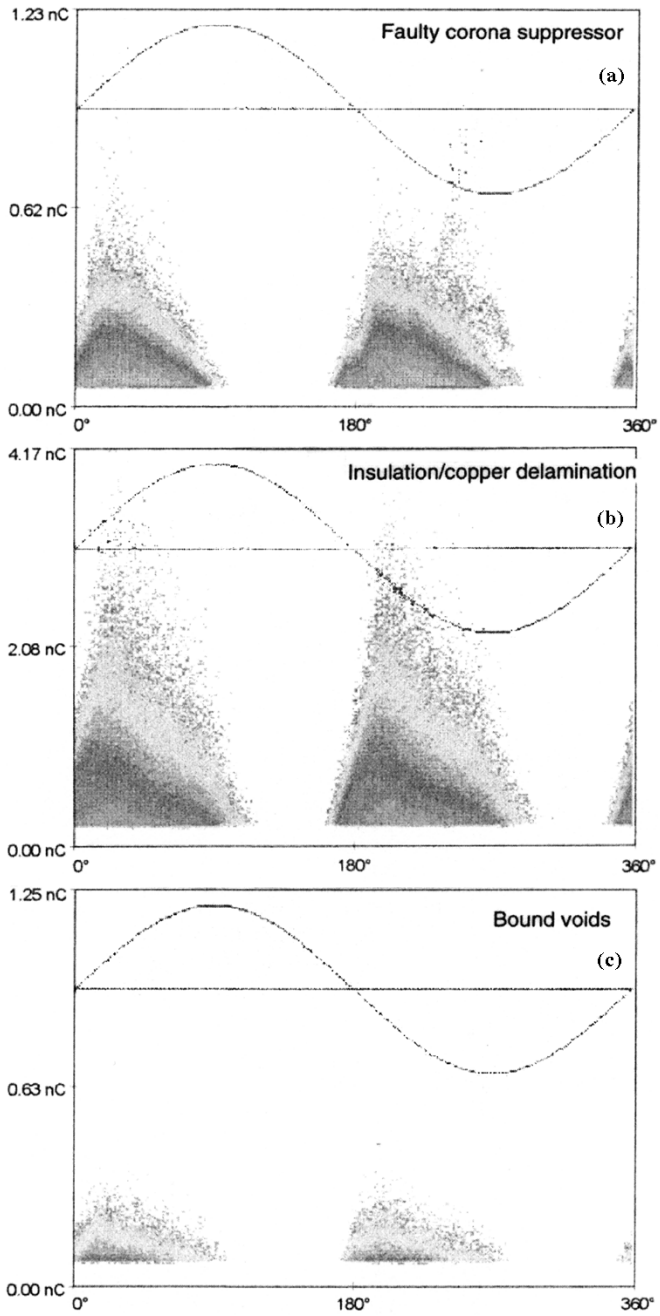

Fig. 12. Representative phase-resolved PD measurements for a bar with (a) faulty corona suppressor, (b) insulation/copper delamination, and (c) bound voids.

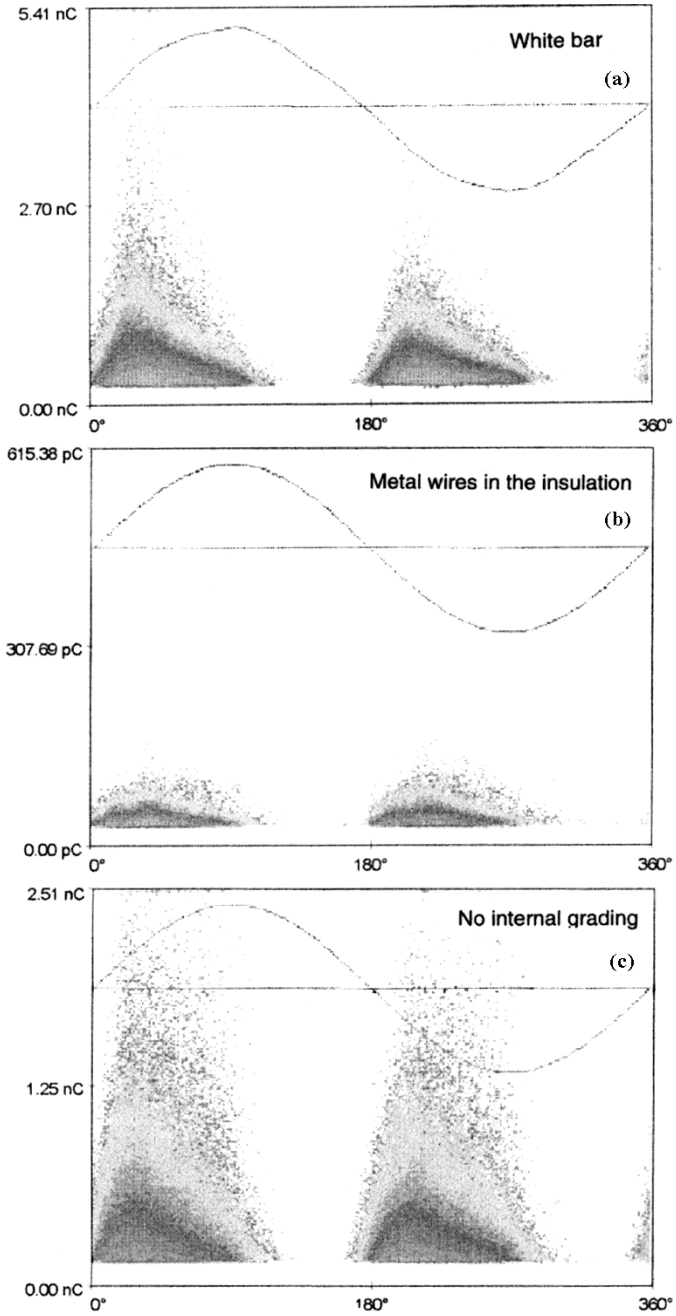

Fig. 13. Representative phase-resolved PD measurements for (a) a white bar, (b) a bar with metal wires in the insulation, and (c) a bar without internal grading.

performance, its validity for lower voltage long-term applications is questionable.

Phase-resolved PD patterns were collected and a representative plot is shown in Fig. 13(c). The immediate observation is that the PD activity is significantly larger than that from a bar with internal grading. In contrast to bars made with internal grading, this activity did not noticeably condition over a period of 16-h energization.

After application of a single hipot, the count rate for this bar increased by more than 50%. Interestingly, however, it was observed that Q_{max} only increased by about 15%. Neither, however, conditioned significantly afterward. This shows the aggravating effect that hipot tests can have on this defect. The hipot test acted to initiate many new sites of activity (*vis a vis* the count rate), without significantly worsening those that already existed.

VII. Numerical Results

In the training stage, we used nine generator bars with various insulation defects and two generator bars with good insulation quality. The bar names and the defect types are tabulated in Table I. From each bar, five PD measurements were collected. A sample PD measurement from each class is shown in Figs. 10, 12, and 13. The number of test samples used for each class is tabulated in Table II. Note that bars TT539 and TT540

TABLE II
NUMBER OF TRAINING SAMPLES FOR EACH CLASS

Class	Number of Measurements
Good Bars	10
Suppresor	5
Metal Wires	5
No Int Grade	10
Cu Delam	5
Puffed	5
Therm & VE	4
Arm Control	4
Slot Discharge	4

TABLE III
CORRELATION THRESHOLDS FOR EACH CLASS

Class	Mean value
Good Bars	0.97
Suppresor	0.96
Metal Wires	0.97
No Int Grade	0.96
Cu Delam	0.98
Puffed	0.98
Therm & VE	0.98
Arm Control	0.98
Slot Discharge	0.95

are combined to form the class of "Good Bars" and TT547B and TT548B are combined to form the class of "No Internal Grading." Therefore, there are nine classes, of which eight are defect classes and one is the good insulation class. Totally, 52 measurements were used in this experiment. Note that the data base can be updated as more samples from the existing classes or new classes become available.

Note that, in our earlier work, we used the same set of measurements to assess various commercially used parameters [6]. These include classical parameters such as the peak discharge magnitude (at a specified count rate) or the overall count rate and a multitude of integrated quantities such as the Normalized Quantity Number (NQN), the Quadratic Rate (QR), the Integrated Charge (IC), the Average Discharge Current (ADC), or the Discharge Power (DP). Statistical parameters included various moments such as the first (average), second (standard deviation), third (skewness), and fourth (kurtosis). More sophisticated approaches involved fractal features.

The representative PD measurement and threshold values were determined for each class with respect to different histogram types and histogram similarity measures. The values of the thresholds for each class with respect to the correlation measure and 2-D histogram are tabulated in Table III. Note that large threshold values indicate that the training samples are statistically homogenous.

We checked the feasibility of the proposed quality assessment method for various histogram similarity measures and histogram types. These include chi-square, correlation, and Kolmogorov–Smirnov tests using 2-D, 1-D, and X- and Y-marginal histograms. The performance of the testing and postprocessing stages is evaluated separately.

For the testing stage, we computed the "defect detection," "false positive rate," and "class identification" power of each histogram similarity measure using 2-D, 1-D, and X- and Y-marginal histograms. The probability of defect detection is defined as the likelihood of classifying a test measurement coming from a defective insulation as defective. Probability of false positive is defined as the likelihood of classifying a test measurement as defective while it is coming from a nondefective insulation, and the identification power is defined as the likelihood of identifying the class type of test measurements correctly. In all of these experiments the α tolerance level is chosen to be 2 unit standard deviation. The performance of each similarity measure and histogram type is tabulated in Tables IV–VII.

Note that it is desirable to have high probability of detection and class identification power and low probability of false positive. Among the type of histograms used, the performance of the 1-D phase-resolved histogram appears to be the best in all categories. The performance of 2-D histogram is also encouraging and has potential for further improvement. However both X- and Y-marginal histograms perform poorly as compared to the first two histogram types, particularly in terms of the probability of false positive and the class identification power.

With respect to the histogram similarity measures, Kolmogorov–Smirnov test2 appears to perform the best in the case of 1-D phase-resolved histogram. Out of 42 measurements, collected from the defective bars, all of them correctly tagged as defective yielding 100% defect detection capability. Out of 10 measurements collected from non defective bars all are tagged as "good bars" yielding 0% probability of false positive. Out of 52 measurements collected from 9 classes all except 1 of them are correctly classified yielding 98% class identification power. The detailed experimental results for each histogram similarity measure and histogram type are summarized in the confusion matrices shown in Tables VIII–XV. The confusion matrices of the X- and Y-marginal histograms are not included since the results are not very significant to present.

Note that in a confusion matrix, the number in the ith row and jth column of this table shows how many samples from class i are classified as class j. For example, in Table VIII, the row titled TT542B shows that one sample is classified as class Grade and four samples are classified as class TT542B. In the case of perfect classification, the confusion matrix is diagonal.

Preliminary experimental results show that the performance of the correlation and Kolmogorov–Smirnov 1 and 2 tests using 1-D phase histograms is excellent. In both 1-D and 2-D histograms, the resolving power of the chi-square test appears to be not as powerful as the other similarity measures. This is particularly evident considering the difference between the bars with metal wire and the nondefective bars. However, the results are encouraging and have potential for further improvement.

TABLE IV
PERFORMANCE OF THE TESTING STAGE USING 1-D PHASE HISTOGRAMS

Test Type	*Defect Detection*	*False Positive*	*Defect ID*
Chi-squares	100%	70%	78%
Correlation	100%	0%	96%
Kolmogorov-Smirnov 1	100%	0%	96%
Kolmogorov-Smirnov 2	100%	0%	98%

TABLE V
PERFORMANCE OF THE TESTING STAGE USING 2-D HISTOGRAM

Test Type	*Defect Detection*	*False Positive*	*Defect ID*
Chi-squares	100%	50%	83%
Correlation	100%	30%	79%
Kolmogorov-Smirnov 1	95%	40%	65%
Kolmogorov-Smirnov 2	93%	30%	69%

TABLE VI
PERFORMANCE OF THE TESTING STAGE USING X-MARGINAL HISTOGRAM

Test Type	*Defect Detection*	*False Positive*	*Defect ID*
Chi-squares	100%	70%	52%
Correlation	98%	30%	69%
Kolmogorov-Smirnov 1	98%	60%	62%
Kolmogorov-Smirnov 2	100%	50%	40%

TABLE VII
PERFORMANCE OF THE TESTING STAGE USING Y-MARGINAL HISTOGRAM

Test Type	*Defect Detection*	*False Positive*	*Defect ID*
Chi-squares	98%	70%	42%
Correlation	98%	60%	35%
Kolmogorov-Smirnov 1	95%	50%	40%
Kolmogorov-Smirnov 2	95%	50%	38%

TABLE VIII
CONFUSION MATRIX FOR THE CHI-SQUARE TEST USING 1-D PHASE HISTOGRAMS

	Supprs	MetalW	NoGrd	CDelam	Puffed	ThrmVE	SDischg	ArmCnt	GBars	Unknwn
Supprs	5									
MetalW	1	4								
NoGrade			10							
CDelam				5						
Puffed	4				1					
ThrmVE	1					3				
SDischg							4			
ArmCnt								4		
GBars		7							3	

We performed extensive experiments to show the feasibility of the postprocessing stage in terms of improving the accuracy of the final decision and providing additional information on the accuracy of the final and intermediate decisions. The results confirm that the proposed postprocessing method is effective in improving the overall accuracy of the classification method.

TABLE IX
CONFUSION MATRIX FOR THE CORRELATION TEST USING 1-D PHASE HISTOGRAMS

	Supprs	MetalW	NoGrd	CDelam	Puffed	ThrmVE	SDschg	ArmCnt	GBars	Unknwn
Supprs	5									
MetalW		5								
NoGrade			10							
CDelam				5						
Puffed		2			3					
ThrmVE						4				
SDischg							4			
ArmCnt								4		
GBars									10	

TABLE X
CONFUSION MATRIX FOR THE KOLMOGOROV–SMIRNOV1 TEST USING 1-D PHASE HISTOGRAMS

	Supprs	MetalW	NoGrd	CDelam	Puffed	ThrmVE	SDschg	ArmCnt	GBars	Unknwn
Supprs	5									
MetalW		5								
NoGrade			10							
CDelam				5						
Puffed		1			4					
ThrmVE						4				
SDischg	1						3			
ArmCnt								4		
GBars									10	

TABLE XI
CONFUSION MATRIX FOR THE KOLMOGOROV–SMIRNOV2 TEST USING 1-D PHASE HISTOGRAMS

	Supprs	MetalW	NoGrd	CDelam	Puffed	ThrmVE	SDschg	ArmCnt	GBars	Unknwn
Supprs	5									
MetalW		5								
NoGrade			9	1						
CDelam				5						
Puffed					5					
ThrmVE						4				
SDischg							4			
ArmCnt								4		
GBars									10	

Based on the training data, we chose the parameters of the Beta distribution function as follows:

$$\gamma = \alpha^2 = 4 \quad \text{and} \quad \beta = -0.322$$

so that Probability $(\Delta > \alpha) = 0.8$.

Here, we only discuss the numerical results of the Kolmogorov–Smirnov test 2 using 1-D phase histograms to illustrate the postprocessing procedure. Table XVI tabulates the distance and the class likelihood probability of each sample coming from the class "suppressor" to the nine classes in the database. The row entitled "Distance1" shows the distance of the ith measurement to the nine classes in terms of unit standard deviations and the row entitled "Prob1" shows the probability of the ith measurement belonging to one of the nine classes in the data base. It is desirable that the distance of the measurements is closest to the class "suppressor" and the class

TABLE XII
CONFUSION MATRIX FOR THE CHI-SQUARE TEST USING 2-D HISTOGRAM

	Supprs	MetalW	NoGrd	CDelam	Puffed	ThrmVE	SDschg	ArmCnt	GBars	Unknwn
Supprs	5									
MetalW		4			1					
NoGrade			9	1						
CDelam			3	2						
Puffed					5					
ThrmVE						4				
SDischg							4			
ArmCnt								4		
GBars		5							5	

TABLE XIII
CONFUSION MATRIX FOR THE CORRELATION TEST USING 2-D HISTOGRAM

	Supprs	MetalW	NoGrd	CDelam	Puffed	ThrmVE	SDschg	ArmCnt	GBars	Unknwn
Supprs	5									
MetalW	1	4								
NoGrade	2		8							
CDelam				5						
Puffed	2				3					
ThrmVE	3					1				
SDischg							4			
ArmCnt	1							3		
GBars		3							7	

TABLE XIV
CONFUSION MATRIX FOR THE KOLMOGOROV-SMIRNOV1 TEST USING 2-D HISTOGRAM.

	Supprs	MetalW	NoGrd	CDelam	Puffed	ThrmVE	SDschg	ArmCnt	GBars	Unknwn
Supprs	4	1								
MetalW		3							2	
NoGrade			6	4						
CDelam			1	4						
Puffed	2				3					
ThrmVE	2					2				
SDischg							4			
ArmCnt	2							2		
GBars		4							6	

likelihood probabilities of the measurements are the highest for the class "suppressor." In this example, four measurements are within 0.59 and one measurement is within 1.46 unit standard deviation of the class "suppressor." The class likelihood probability of the measurements is at least 95% for the close ones and 86% for the other ones. Therefore, all five measurements are classified as class "suppressor" with an average likelihood of 94%. However, if we look at the third measurement, we see that it is within 2.11 unit standard deviations of the class "thermaVE" with a likelihood probability of 0.79. Similarly, other measurements are also within nonnegligible neighborhood of the class "thermaVE." This yields an average 72% likelihood probability that the test bar may be of class "thermaVE."

Table XVII summarizes the likelihood probabilities of the bars for each class. Although all the test bars have the highest class likelihood probability for the true class, some bars exhibit significant similarity to more than one class. For example in the case of bar with metal wire, it was found that the test bar belongs

TABLE XV
CONFUSION MATRIX FOR THE KOLMOGOROV–SMIRNOV2 TEST USING 2-D HISTOGRAM

	Supprs	MetalW	NoGrd	CDelam	Puffed	ThrmVE	SDschg	ArmCnt	GBars	Unknwn
Supprs	5									
MetalW		2							3	
NoGrade	3		7							
CDelam				5						
Puffed	3				2					
ThrmVE	3					1				
SDischg							4			
ArmCnt	1							3		
GBars		3							7	

TABLE XVI
DISTANCES PAND CLASS LIKELIHOOD OF THE MEASUREMENTS FROM CLASS "SUPPRESSOR" FOR THE KOLMOGOROV–SMIRNOV2 TEST USING 1-D PHASE HISTOGRAMS

	Supprs	MetalW	NoGrde	CuDelam	Puffed	ThermVE	SDischg	ArmCnt	GBars
Distance1	1.46	2.49	5.27	6.29	2.45	3.80	4.25	4.07	2.65
Prob1	0.86	0.73	0.00	0.00	0.74	0.38	0.00	0.00	0.71
Distance2	0.59	4.21	3.44	3.86	2.06	2.18	2.34	3.40	5.41
Prob2	0.95	0.00	0.53	0.34	0.79	0.78	0.75	0.54	0.00
Distance3	0.55	4.16	3.26	3.49	1.97	2.11	2.36	3.03	5.35
Prob3	0.95	0.00	0.58	0.52	0.80	0.79	0.75	0.63	0.00
Distance4	0.54	4.04	3.55	3.77	1.90	1.88	2.28	3.10	5.20
Prob4	0.95	0.00	0.50	0.40	0.81	0.82	0.76	0.62	0.00
Distance5	0.51	4.19	3.43	3.65	1.96	1.86	2.13	3.23	5.37
Prob5	0.96	0.00	0.53	0.46	0.81	0.82	0.78	0.59	0.00

TABLE XVII
CLASS LIKELIHOOD OF EACH BAR FOR THE KOLMOGOROV–SMIRNOV2 TEST USING 1-D PHASE HISTOGRAMS

	Supprs	MetalW	NoGrde	CuDelam	Puffed	ThermVE	SDischg	ArmCnt	GBars
Grade	**0.94**	0.15	0.43	0.34	0.79	0.72	0.61	0.48	0.14
TT542	0.72	**0.93**	0.00	0.00	0.82	0.13	0.00	0.56	0.88
TT547B	0.24	0.00	**0.93**	0.84	0.00	0.00	0.00	0.00	0.00
TT548B	0.47	0.00	**0.93**	0.60	0.00	0.00	0.00	0.00	0.00
TT555	0.70	0.00	0.84	**0.93**	0.00	0.00	0.00	0.00	0.00
TT595	0.88	0.79	0.32	0.00	**0.93**	0.75	0.11	0.76	0.57
2E18	0.90	0.32	0.10	0.14	0.82	**0.93**	0.64	0.38	0.14
2G17	0.87	0.00	0.46	0.40	0.56	0.56	**0.93**	0.09	0.00
2G18	0.81	0.66	0.44	0.00	0.82	0.00	0.00	**0.93**	0.27
TT539B	0.70	0.90	0.00	0.00	0.78	0.00	0.00	0.32	**0.93**
TT540B	0.61	0.89	0.00	0.00	0.72	0.00	0.00	0.08	**0.94**

to the class of "metal wires" with 93% probability whileit may also belong to the class of nondefective bars with 88% probability.

The class likelihood probabilities may help the user to decide if additional measurements and testing are needed before the final decision on the insulation equipment is called.

VIII. CONCLUSION

In this paper, we presented a new statistical analysis method of PD measurements. This analysis may be used for the quality assessment of electrical insulation systems, particularly, high-voltage motors and generators. The method is based on a supervised classification approach which utilizes histogram sim-

ilarity analysis. The motivation for choosing histogram similarity measures is twofold. First, the phase-resolved PD measurements themselves are, in fact, 2-D histograms. Therefore, a histogram-matching-based approach suits the very nature of the data. Second, histogram similarity measures combine the typical statistical parameters in a statistically powerful and rigorous manner, such as mean, variance, and higher order moments, employed in the analysis of PD measurements.

In our approach, we treat the phase-resolved PD data as four different kinds of histograms: 1) 2-D histogram; 2) 1-D histogram; 3) X-marginal histogram; and 4) Y-marginal histogram. Among the histogram similarity measures, we studied: 1) sample correlation; 2) Kolmogorov–Smirnov distance 1; 3) Kolmogorov–Smirnov distance 2; and 4) chi-square distance.

Further, we developed a postprocessing method which provides likelihood of any test equipment belonging to one of the classes in the data base. As a result, the accuracy of the final classification results are improved and quantified. Such an approach facilitates soft decision making and guides users for further action.

The discrimination capability of the histogram types and distance measures were appraised using over 50 laboratory patterns from nine different classes. Our results suggest that Kolmogorov–Smirnov 2 test using 1-D phase histograms performed the best, yielding 100% defect detection, 0% false positives, and 98% class identification power. In the case of 2-D histograms, all similarity measures performed comparably and are encouraging, but not as good as 1-D phase histograms. In the case of X- and Y-marginal histograms, all similarity measures performed poorly as compared to 2-D and 1-D histograms. Results based on 2-D and marginal histograms can be improved by an appropriate combination of these techniques.

Our preliminary experimental results demonstrate that the method shows strong potential for detecting and identifying insulation defects. The approach could be applied as a statistical process control tool during manufacturing of individual bars, windings, or complete machines. Finally, the approach can be utilized for online or offline testing of aged machinery to quantify the degradation in electrical insulation.

ACKNOWLEDGMENT

The author is grateful to J. R. Krahn and K. Rao of General Electric Company for performing the experiments presented in this study. The author also would like to thank the anonymous reviewers who helped improve the technical content and presentation of this paper.

REFERENCES

[1] *IEEE Trial-Use Guide to the Measurement of Partial Discharges in Rotation Machinery*, IEEE Std 1434-2000.

[2] E. Gulski and A. Krivda, "Neural networks as a tool for recognition of partial discharges," *IEEE Trans. Elect. Insulation*, vol. 28, pp. 984–1001, Dec. 1993.

[3] E. Gulski and L. Niemeyer, "The importance of statistical characteristics of partial discharge data," *IEEE Trans. Elect. Insulation*, vol. 27, pp. 60–69, Feb. 1992.

[4] E. Gulski, *Computer Aided Recognition of Discharges Using Statistical Tools*. Delft, The Netherlands: Delft Univ. Press, 1991.

[5] L. Niemeyer, L. Pietronero, and H. J. Wiesman, "Fractal dimension of dielectric breakdown," *Phys. Rev. Lett.*, vol. 52, no. 12, pp. 1033–1036, 1984.

[6] J. R. Krahn, B. Yazici, and K. Rao, "Statistical pattern recognition techniques for defect analysis of large AC machine insulation systems," in *CIGRE/EPRI Colloq. Maintenance and Refurbishment of Utility Turbogenerators, Hydrogenerators, and Large Motors*, Florence, Italy, Apr. 1997.

[7] B. Yazici and J. R. Krahn, " Statistical pattern analysis methods of partial discharge measurements in high voltage insulation," U.S. Patents 6 088 658 and 6 192 317, July, 11 2000 and February 20, 2001.

[8] R. B. D'Agostino and M. A. Stephens, Eds., *Goodness-of-Fit Techniques*. ser. III: Statistics, Textbooks, and Monographs. New York: Marcel Dekker, 1986, vol. 68.

[9] C. Hudon, R. Filkens, and J. R. Krahn, "Discrimination capability of PD analysis for assessment of generator windings," presented at the EPRI Turbine Generator Workshop, Milwaukee, WI, Aug. 1995.

[10] G. C. Stone, "Partial discharge measurements to assess rotation machine insulation conditions," in *Proc. IEEE Int. Symp. Electrical Insulation*, Montreal, QC, Canada, June 1996, pp. 19–23.

[11] D. Gross, "On-line partial discharge diagnosis on large motors," in *Proc. IEEE Conf. Electrical Insulation and Dielectric Phenomena*, Oct. 2002, pp. 474–477.

[12] H. Zhu, V. Green, D. Huynh, and L. Ravenscroft, "How to identify stator insulation problems using on-line partial discharge analysis," in *Proc. IEEE Int. Symp. Electrical Insulation*, Apr. 2000, pp. 506–511.

[13] *High Voltage Test Techniques—Partial Discharge Measurements*, IEC Standard 60270, 2000.

[14] R. Von Mises, *Mathematical Theory of Probability and Statistics*. New York: Academic, 1964.

[15] G. Fasano and A. Franceschini, *Astron. Soc. Monthly Notice*, vol. 225, pp. 155–170, 1987.

Birsen Yazici (M'97) received B.S. degrees in electrical engineering and mathematics from Bogazici University, Istanbul, Turkey, in 1988, and the M.S. degree in mathematics and the Ph.D. degree in electrical engineering from Purdue University, West Lafayette, IN, in 1990 and 1994, respectively.

From September 1994 until 2000, she was a Research Engineer at the General Electric Company Global Research Center, Schenectady NY. During her tenure in industry, she worked on transportation, industrial, and medical imaging systems. From January 2001 until June 2003, she was with the Electrical and Computer Engineering Department, Drexel University, Philadelphia, PA. In July 2003, she joined the Electrical, Computer and Systems Engineering Department, Rensselaer Polytechnic Institute, Troy, NY. Her research interests span the areas of statistical signal and image processing, time-series analysis, inverse problems in imaging, biomedical optics, and computer methods in industrial applications. She is the holder of 12 U.S. patents.

Dr. Yazici received the the 1997 Second Prize Paper Award from the IEEE TRANSACTIONS ON INDUSTRY APPLICATIONS.